MASTER OF PHILOSOPHY, Modelling of Materials

Friday 25 April 2003   9 – 12

MODELLING OF MATERIALS (2) – possible answers

SECTION A

1(a).   The result follows from the fact that $\mathbf{a}_i.\mathbf{a}_j^* = 1$ when $i = j$, and $\mathbf{a}_i.\mathbf{a}_j^* = 0$ when $i \neq j$

The required value is zero since the vectors are normal.

1(b).   The *hydrostatic* stress is calculated by the mean of the diagonal stresses and represents a stress state in which each primary direction is subjected to an equal stress and gives volume change without shape change. The *deviatoric* component represents the stresses giving rise to shape change.

$$\begin{pmatrix} \sigma_1 & 0 \\ 0 & 0 \end{pmatrix} = \begin{pmatrix} \sigma_1/2 & 0 \\ 0 & \sigma_1/2 \end{pmatrix} + \begin{pmatrix} \sigma_1/2 & 0 \\ 0 & -\sigma_1/2 \end{pmatrix}$$

hydrostatic   +   deviatoric

1(c).   For a Lennard-Jones potential the interaction energy, U, has the form:

$$U = \frac{1}{2} \sum_{ij} \left(-\frac{A}{r_{ij}^6} + \frac{B}{r_{ij}^{12}} \right)$$

where the factor of $^1/_2$ exists to remove double-counting terms.

The Lennard-Jones potential is a simple pair potential, and consists of an attractive term ($^{-A}/r^6_{ij}$) and a repulsive term ($^B/r^{12}_{ij}$). We know that the Van der Waals interaction between two atoms is attractive, and arises from the interaction between the atoms' dipoles. Each dipole generates an electric field which is proportional to $^1/r^3_{ij}$ and so the mutual interaction is proportional to $^1/r^6_{ij}$, hence the form of the attractive term (negative implies an attractive force).

The repulsive term must be present to prevent the atoms from collapsing into each other. It is convenient to choose a polynomial ($^1/r^m$) form for this as well, and the power m must be chosen so that the repulsive force is negligible compared to the attractive force at long range (since the net long-range force should be attractive), but dominates at short-range (to prevent the atoms collapsing into each other). This means $m > 6$. The choice of $m = 12$ is fairly arbitrary, but convenient.

Important features of the sketch: U is large (tends to $+\infty$) for small r; slope is large and negative for small r; there is a minimum; slope is positive for large r, and tends to zero as r tends to $+\infty$.

1(d).   The Born-Oppenheimer approximation makes two assumptions: firstly that nuclei can be treated as classical particles, and secondly that they move so slowly that electrons will always be in their equilibrium state for any given nuclear configuration. It is usually justified because the nuclei are much more massive than the electrons (by between 3 and 5 orders of magnitude) - the lighter electrons can respond much more rapidly to a change in nuclear configuration than can the nuclei themselves, and the nuclei are so massive that the classical approximation is usually good.

Cases where the Born-Oppenheimer approximation would be poor include: many situations involving hydrogen (helium, lithium...), because hydrogen is light enough that the classical approximation is often poor. This is illustrated by the large zero-point motion of hydrogen; any system where electron-phonon interactions are important, since it ignores any (direct) interaction between electronic and nuclear motion; any quantum phenomenon of the nuclei, such as Bose condensation.

```
1(e).  implicit none

       integer i, j, k

       real eps(3,3,3)

       do 10 i = 1, 3

          do 10 j = 1, 3

             do 10 k = 1, 3

                eps(i,j,k) = 0.0

   10  continue

       eps(1,2,3) = 1.0

       eps(2,3,1) = 1.0

       eps(3,1,2) = 1.0

       eps(1,3,2) = -1.0

       eps(2,1,3) = -1.0

       eps(3,2,1) = -1.0
```

1(f). *Homogeneous nucleation* is the generation of a new phase in a parent phase without any catalysis by heterogeneities in the parent phase. In the simplest model, the nucleus is spherical. It arises from statistical fluctuations in the parent phase. *Heterogeneous nucleation* is where nucleation is catalysed, for example on the surface of a foreign particle. The nucleus takes the form of a spherical cap on the surface. The balance of interfacial energies determines the contact angle. The critical radius of curvature of the solid-liquid interface is the same for homogeneous and heterogeneous nucleation, but the volume of the critical nucleus can be much smaller in the latter case. Correspondingly, the work of nucleation can be much smaller.

The lack of purity or perfection in most real systems gives plenty of opportunity for heterogeneous nucleation, and because it is easier it almost always dominates.

Homogeneous nucleation can be detected, for example, in droplet emulsion experiments. In these a liquid (*e.g.* mercury) is dispersed in a carrier fluid. Once the number of dispersed droplets exceeds the number of nucleating heterogeneities, there must be some droplets without nucleants; these show much larger undercoolings before solidification is nucleated, and in the ideal case the nucleation in these droplets is homogeneous.

1(g). The DREIDING force field is represented by the following potential energy function

$$V = \frac{k_b}{2}\left(r_{ij} - r_0\right)^2 + \frac{k_\theta}{2}\left(\theta_{ijk} - \theta_0\right)^2 + \frac{k_\varphi}{2}\left(1 + \cos 3\varphi_{ijkl}\right) + D_0\left\{\left(\frac{R_0}{r_{ij}}\right)^{12} - 2\left(\frac{R_0}{r_{ij}}\right)^6\right\} + \frac{q_i q_j}{4\pi\varepsilon_0 r_{ij}}$$

where the k are force constants, r_{ij} the interatomic separations, θ_{ijk} the angles between adjacent triplets of bonded atoms, φ_{ijkl} the dihedral angles between adjacent quartets of bonded atoms, D_0 is the well-depth and R_0 the equilibrium separation for the van der Waals interactions, and q the electrostatic charges on the atoms. The first three terms are called bonded terms, and represent the internal degrees of freedom of the molecule, and the last two terms are the non-bonded terms, and represent the interactions between molecules. (Candidates are not expected to write out this function – but it's here to illustrate the basis of the question.)

To test the paramaterisation of the bonded terms, one could compare force constants with those obtained from *ab intio* quantum calculations or calorimetric data. Equilibrium bond lengths and angles can be derived from crystallographic data. Torsional force constants are much harder to measure, but can be inferred indirectly from the stiffness of the macromolecule by measuring the Kuhn length or characteristic ratio via scattering techniques. Ultimately, the accuracy of the parameterisation rests in being able to predict bulk properties such as elastic moduli, melting temperature, glass transition temperature, etc, and so the best answers will include a brief discussion of how force field parameters affect equation of state in very simple systems, such as binary Lennard-Jones fluid, by comparing simulated and experimental phase diagrams.

1(h).   Axisymmetric meshes are used for problems which have rotational symmetry, with no variation in the circumferential direction, *i.e.* in polar coordinates z, r, θ the variables are functions of z, r only. The mesh is defined in the z, r plane, with the axis of rotation in the z-direction.

A graded mesh is one in which adjoining elements progressively change in size, with smaller elements being used in regions where the variables vary rapidly with respect to position and/or time.

Linear elements are those in which the dependent variable (*e.g.* temperature) is made to vary linearly between the nodes of the element. Quadratic elements allow second order interpolation between the nodes.

Automatic remeshing is where the FE solver automatically refines the mesh locally in response to the appearance of steep gradients in the dependent variables (*e.g.* local intense deformations or cooling in a forming process, where the dies make fresh contact with the workpiece).

1(i).   Equiaxed growth in a pure metal can show morphological instabilities when there is a negative temperature gradient in the liquid ahead of the solid-liquid interface. This is because a small perturbation at the interface ends up in even more supercooled liquid, so that the interface becomes unstable.
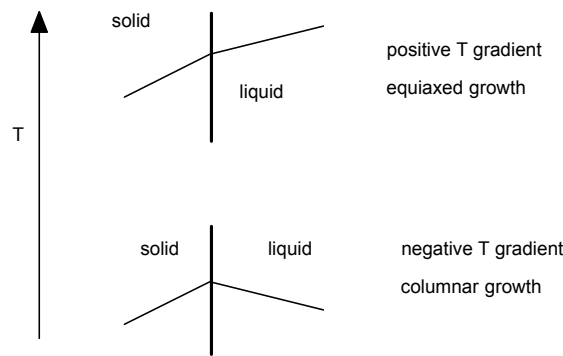
Fig. 1. The conditions needed for dendrite formation in a pure liquid.

1(f).   Lines of constant value of merit index M have slope -1 on $\log(\sigma_y) - \log(\lambda)$ plot. Move line up to top right to identify material classes with highest values of M: carbon steels and aluminium alloys.
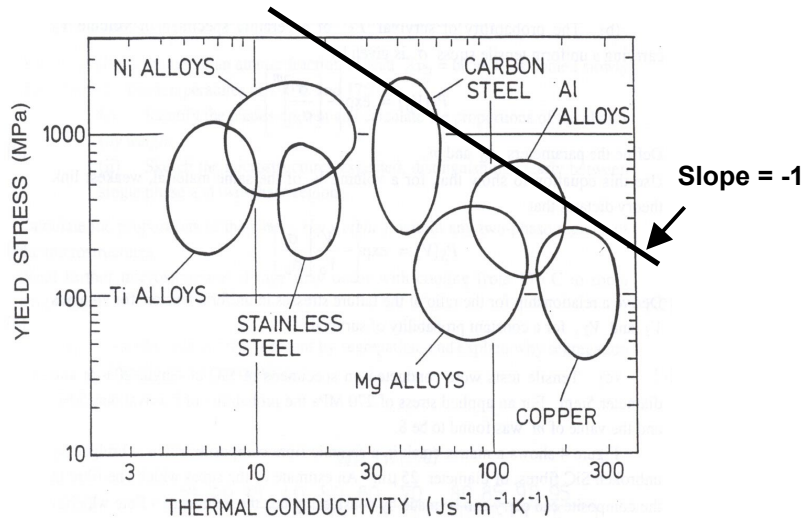
Fig. 2. Selection chart, showing line of constant value merit index: $M = \lambda\sigma_y = $ constant

SECTION B

2. The free particle:

For a free particle V=0 everywhere, which means the Schrodinger equation reduces to:

$$-\frac{1}{2}\frac{d^2\psi}{dx^2} - E\psi = 0$$

There are two basic techniques we could use to solve this:

Method 1: This is a second-order ordinary differential equation. To solve, we form the auxiliary equation:

$$-\frac{1}{2}\lambda^2 - E = 0$$

which gives $\lambda = \pm i\sqrt{2E}$

so our complementary function (and general solution, since RHS is zero) is

$$\psi(x) = \alpha e^{i\sqrt{2E}x} + \beta e^{-i\sqrt{2E}x}$$

where α and β are constants of integration.

Method 2: We note that this is a simple harmonic equation, and therefore must have solutions of the form:

$$\psi(x) = A\sin kx + B\cos kx$$

where A and B are constants of integration. Differentiating this and substituting into Schrodinger's equation gives:

$$-\frac{1}{2}k^2\psi(x) = -E\,\psi(x)$$

i.e. $k = \pm\sqrt{2E}$

N.B. the students will have seen this solved by taking the positive square root only. At first sight this is not the fully general solution, but the symmetry of sine and cosine means that these two apparently different solutions are in fact dependent. It is sufficient to choose one of these solutions.

Thus the general solution is: $\psi(x) = A\sin(\sqrt{2E}x) + B\cos(\sqrt{2E}x)$

The infinite potential well:

To keep the equations tidy, we use $k = \sqrt{2E}$. Inside the well our wavefunction is the same as that of a free particle, *i.e.*

$$\psi(x) = A\sin kx + B\cos kx$$

Outside the well the potential energy is infinite, and so the wavefunction must be zero. This leads to two boundary conditions: $\psi(a) = 0$ and $\psi(-a) = 0$.

Substituting for $\psi(x)$ we get: $A \sin ka + B \cos ka = 0$ (1)

and $A \sin(-ka) + B \cos(-ka) = 0$ (2)

i.e. $-A \sin ka + B \cos ka = 0$ (3)

Adding equations (1) and (3) gives: $2B\cos(ka) = 0$

i.e. $B = 0$, or $k = \dfrac{(2n-1)\pi}{2a}$ where n is a positive integer (i.e. k is an odd multiple of $\pi/_{2a}$)   (4)

Subtracting equations (1) and (3) gives: $2A\sin(ka) = 0$

i.e. $A = 0$, or $k = \dfrac{n\pi}{a}$ where n is a positive integer (i.e. k is an even multiple of $\pi/_{2a}$)   (5)

It is convenient to amalgamate equations (4) and (5): $k = \dfrac{m\pi}{2a}$ where m is an integer,

and we note that even m implies a sine solution for $\psi(x)$ and odd m a cosine solution for $\psi(x)$.

Putting these two solutions together we see that $A = 0$, $B = 0$ is a trivial solution and can be discounted (it represents no particle in the well), and the two conditions on k cannot be satisfied simultaneously. This leaves two possible sets of solutions:

$$\psi(x) = A\sin(\frac{m\pi x}{2a}) \quad \text{where } m \text{ is even, or}$$

$$\psi(x) = B\cos(\frac{m\pi x}{2a}) \quad \text{where } m \text{ is odd.}$$

Since $k = \sqrt{2E}$ we have:

$$E = \frac{1}{2}k^2$$

$$= \frac{m^2\pi^2}{8a^2} \tag{6}$$

where m is an integer, even m from the sine solution for $\psi(x)$ and odd m coming from the cosine solution.

Finally, we need to normalise the wavefunctions such that:

$$\int_{-a}^{a} |\psi(x)|^2\, dx = 1$$

$$i.e. \quad 1 = \int_{-a}^{a} A^2 \sin^2\left(\frac{m\pi x}{a}\right) dx$$

$$= \int_{-a}^{a} \frac{A^2}{2}\left(1 - \cos\left(\frac{2m\pi x}{a}\right)\right) dx$$

$$= \frac{A^2}{2}\left[x - \frac{a}{2m\pi}\sin\left(\frac{2m\pi x}{a}\right) \right]_{x=-a}^{x=a}$$

$$= \frac{A^2}{2}[(a) - (-a)]$$

$$= aA^2 \qquad i.e. \qquad A = \sqrt{\frac{1}{a}}$$

and normalising the second form for $\psi(x)$ gives:

$$1 = \int_{-a}^{a} B^2 \cos^2\left(\frac{m\pi x}{2a}\right) dx$$

$$= \int_{-a}^{a} \frac{B^2}{2}\left(1 + \cos\left(\frac{m\pi x}{a}\right)\right) dx$$

$$= \frac{B^2}{2}\left[x - \frac{a}{m\pi}\sin\left(\frac{m\pi x}{a}\right) \right]_{x=-a}^{x=a}$$

$$= \frac{B^2}{2}[(a) - (-a)]$$

$$= aB^2 \qquad i.e. \qquad B = \sqrt{\frac{1}{a}}$$

It is clear from equation (6) that the ground state energy is the $m = 1$ state, which has energy $E_0 = \pi^2/8a^2$ and arises from the cosine solution:

$$\psi(x) = \psi_0(x) = \sqrt{\frac{1}{a}}\cos\left(\frac{\pi x}{2a}\right)$$

and the first excited state corresponds to $m = 2$, which has energy $E_1 = \pi^2/2a^2$ and comes from the sine solution:

$$\psi(x) = \psi_1(x) = \sqrt{\frac{1}{a}}\sin\left(\frac{\pi x}{a}\right)$$

$$|\psi_0(x)|^2 = \frac{1}{a}\cos^2\left(\frac{\pi x}{2a}\right)$$

Thus the moduli-squared are:

$$|\psi_1(x)|^2 = \frac{1}{a}\sin^2\left(\frac{\pi x}{a}\right)$$

The important features of the sketch for $|\psi_0(x)|^2$ are: cosinusoidal; maximum at $x = 0$, where $|\psi_0(x)|^2 = 1/a$; $|\psi_0(-a)|^2 = |\psi_0(a)|^2 = 0$

and the important features of the sketch for $\left|\psi_1(x)\right|^2$ are: sinusoidal; zero at $x = 0$; maxima at $x = \pm^a/_2$, where $\left|\psi_1(x)\right|^2 = {}^1/_a$; $\left|\psi_1(-a)\right|^2 = \left|\psi_1(a)\right|^2 = 0$

The difference between these probability distributions and that of a classical particle is that a classical particle is equally likely to be anywhere in the well, *i.e.* the probability distribution is uniform in the well. For these quantum states the probability distribution is sharply peaked, and goes to zero for certain values of x..

3.
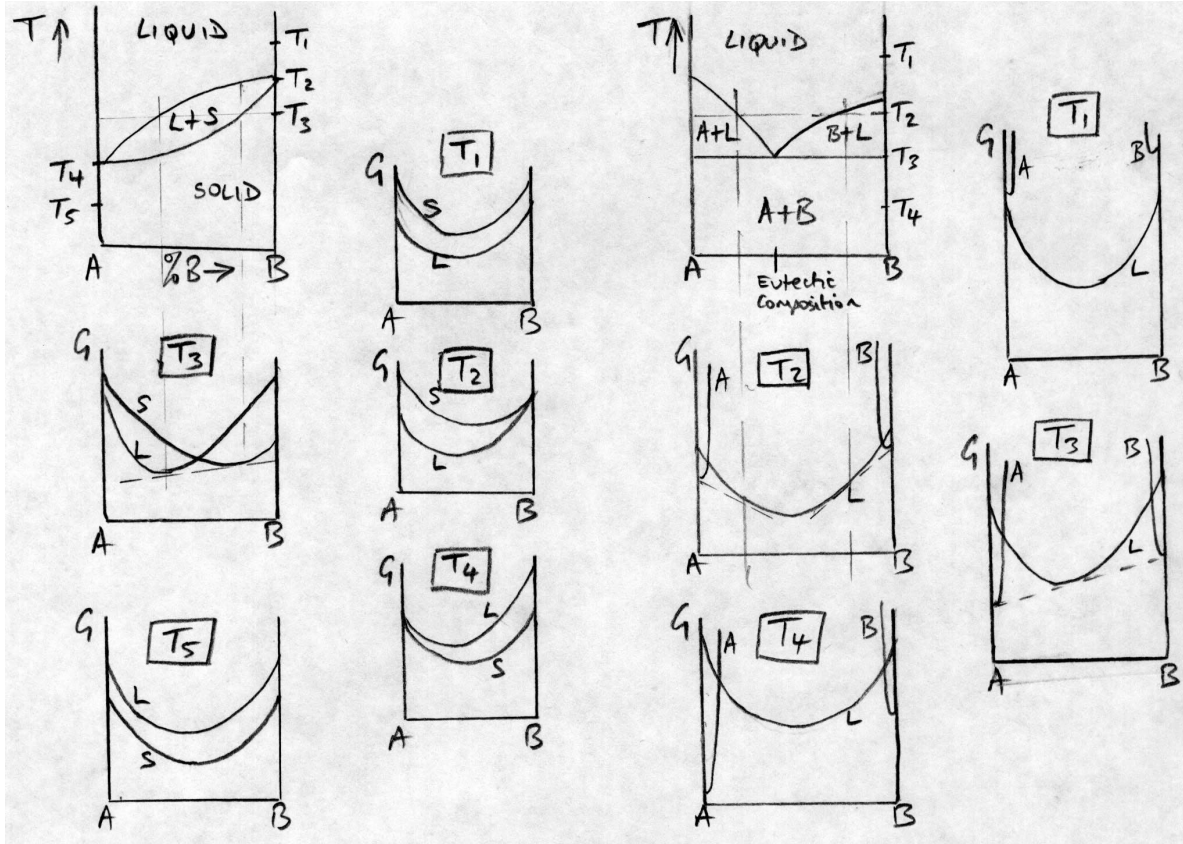
Fig. 3. (a) Complete solid solution   (b) Eutectic system: (T_3 = eutectic temperature)

B in solid solution in *A*: α-phase

A in solid solution in *B*: β-phase

Free energy curves of solid solutions (α and β) are broader.
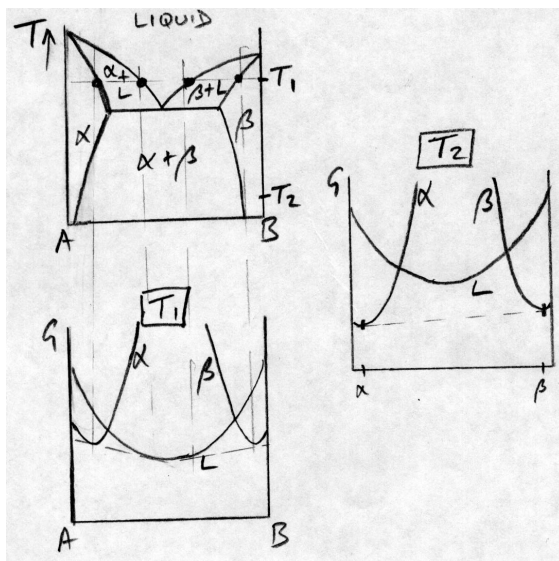
Fig. 4. Increased solid solubility.

4.   Since the atomistic structure of the Pluronics molecules is irrelevant for the purposes of this question, a suitable discrete element (as opposed to continuous density) representation would be a system of spherical beads joined by harmonic springs, denoted by $A_xB_yA_x$ (or equivalent diagrammatic sketch). In this case, the 'A'-type beads represent groups of PEO monomers, and 'B'-type beads represent groups of PPO monomers. At this stage, we cannot say how many PEO or PPO monomers correspond to each A or B unit, but each bead must be sufficiently large that it can be considered to be freely jointed to its neighbours (*i.e.* the coarse-grained chain is Gaussian). We know that the chain architecture is such that the central B block (consisting of y B units) is surrounded on either side by symmetric A blocks (each consisting of x A units). Therefore, two natural structural parameters of the coarse-grained model are the values of x and y. These would be proportional to n and m in the atomistic model.

Furthermore, we must consider the nature of the chemical interactions between A and B beads. Generally, the PPO portions of the copolymer are hydrophobic and PEO is hydrophilic, which will drive phase separation of a mixture of Pluronics, water and a hydrophobic substance (e.g. oil, dirt or a drug molecule). We can characterise the interactions of the Pluronics molecules by just three parameters: ε_{AA}, ε_{BB}, which represent self-interactions of PEO and PPO, and ε_{AB}, which represents the interaction between PEO and PPO beads. By setting $\varepsilon_{AB} > \varepsilon_{AA} = \varepsilon_{BB}$, we can drive the system into a phase-separated state. The interaction parameters can also be mapped onto the Flory-Huggins χ parameter in order to reproduce the correct mixing behaviour for PPO and PEO homopolymers.

As stated in the answer to the first part of the question, the A and B beads must be freely-jointed. Hence, their size must be of the order of one Kuhn length. Since the chain dimensions of the coarse-grained blocks must be similar to that of the atomistic blocks, then:

$$C_\infty nl^2 = Na_K^2$$

where $C_\infty = a_k / l$ is the characteristic ratio of each block component, n is the number of monomer units in each block, N is the number of coarse-grained beads in each block and a_k is the Kuhn length of each block component. Thus, rearranging the above expression, we obtain:

$$\frac{n}{N} = \frac{a_K^2}{C_\infty l^2} = C_\infty \Rightarrow N = \frac{n}{C_\infty}$$

and so the number of coarse-grained beads in each block is simply the number of monomer units divided by the characteristic ratio of each block component. For PEO_{13}-PPO_{30}-PEO_{13}, this gives $x = 13/4.25 = 3$ and $y = 30/5.05 = 6$ (rounded to nearest significant digit).

The above discrete element coarse-grained models could be turned into a mesoscale computer simulation using either a lattice-based Monte Carlo technique or by using particulate coarse-grained molecular dynamics. One example of the former method described in lectures was the use of a face-centred lattice in which the distance between lattice points corresponds to the Kuhn length. One example of the latter method described in lectures was dissipative particle dynamics (DPD), which is based on solving Newton's equations for a system of coarse-grained particles interacting via binary pair-wise interactions including dissipative and random terms. Since momentum is strictly conserved in DPD, it reproduces hydrodynamic behaviour that is not captured by the lattice MC method. One would expect these mesoscale simulations to describe the equilibrium configurational properties of coarse-grained polymers quite well (*i.e.* character-istics of phase-separated morphology) but not the smaller length scale features. Hence, conventional molecular dynamics could be used in conjunction with mesoscale simulations to calculate the Kuhn length and interaction parameters required by the latter as an input.

5.   Attributes specific to metal cutting which can be used for initial screening are:
       - compatibility with material to be cut
       - maximum thickness
       - limiting curvature which can be cut

Many design requirements can only be addressed by considering *combinations* of parameters of the design, material and process (rather than singly). A further complication is that the parameters needed to evaluate a given requirement are often specific to each process variant (rather than being generic across all processes).

Examples of the above in metal cutting:
       (a) Cutting speed cannot be identified as a simple process attribute for each variant, since it depends on: material thickness (a design parameter), material type (a material parameter), and a set of process parameters (specific to each process).
       e.g. for laser cutting: power and beam radius, or for water jet: pressure and jet diameter.

(b) "Kerf angle" (a measure of the quality of the cut edges) is another parameter which cannot be usefully stored as a generic attribute of all cutting processes, as it depends on the material being cut, its thickness, and the process operating conditions.

Examples of design requirements from other manufacturing tasks which require complex analysis rather than simple screening:

- aluminium casting: ability to completely fill fine features is a function of mould type, alloy fluidity and shape/ size of the feature;

- steel welding: ability to meet a maximum hardness target depends on the joint thickness, steel hardenability, and process heat input.

Examples of application of process modelling in selection:

Cutting: estimating cutting speed (for cost modelling) *e.g.* laser processes – heat balance/heat flow models; empirical power-law models for water-jet cutting.

Welding: estimating max. HAZ hardness, *e.g.* arc welding – heat flow models to estimate cooling rate; semi-empirical/physically-based models for hardenability to predict % martensite and resulting maximum hardness.

SECTION C

6. The MMC method is based on the principle of thermal importance sampling, *i.e.* that the thermodynamic properties of a system can be calculated by an arithmetic average over states sampled from a Boltzmann distribution. These states are generated via a stochastic algorithm (Markov chain), with transitions between states being determined by an acceptance probability that depends on the relative energy of the initial and final states. In order to produce accurate averages, the MMC assumes ergodicity, *i.e.* that each state must in principle be accessible from any other state. Since states are sampled from a distribution, there is no proper time in a MMC simulation and so it should only strictly be used to generate equilibrium configurations and properties.

The Metropolis algorithm can be summarised as follows:

1. Start with system in arbitrarily chosen state μ and evaluate the internal energy E_μ
2. Generate a new state ν by a small ergodic perturbation to state μ and evaluate E_ν
3. If $E_\nu - E_\mu < 0$, then accept the new state. If $E_\nu - E_\mu > 0$, then accept the new state with probability $\exp[-\beta(E_\nu - E_\mu)]$

Return to step 2 and repeat until equilibrium is achieved (i.e. thermodynamic state function of interest has converged to steady-state value when averaged over all configurations)

For a 2D polymer chain with excluded volume on a square lattice, with interaction energy ε associated with each pair of nearest-neighbour non-bonded sites, the energy of each configuration is infinite if there are any overlapping sites, and computably finite if there are any nearest-neighbour non-bonded sites. Any number of move sets could potentially be used, provided they are ergodic, but the simplest choice is one in which the chain ends can move to any free adjacent sites (no diagonal moves allowed) and any kinks in the chain can be 'flipped' to their mirror image (if permitted by excluded volume). More sophisticated 'crank-shaft' motions can be introduced to speed up equilibration, at the expense of loss of information about dynamics.

(i)   (ii)

Fig. 5. For the figure shown in the question, the initial state (i) has energy 2ε, with the two site-site interactions shown in gray, and the final state (ii) has energy ε, so transition probability is $\exp[-\beta(E_f - E_i)] = \exp(\beta\varepsilon)$. This probability will be the same regardless of the route taken from initial to final state, as the MMC method is path-independent.

The Rosenbluth configuration bias scheme is a method for improving the efficiency of the standard MMC algorithm for dense systems of macromolecules by biasing the trial configurations towards those that are likely to be accepted by the Metropolis criterion. Adjusting the Metropolis criterion to select trial states on the basis of their Rosenbluth factors rather than difference in energies then restores the unbiased canonical thermodynamic averages. The algorithm for regenerating the chain configuration on lattice with co-ordination number k ($k = 4$ for the primitive square lattice given in question) can be summarised as follows:

    1. Insert first atom at point X on the lattice and compute its energy.
    2. The next segment has k possible directions, so select a particular direction (label it n) with probability $p_i(n)$:

$$p_i(n) = \exp\{-\beta E_i(n)\} / w_i(n), \text{ where } w_i(n) = \sum_{j=1}^{k} \exp\{-\beta E_i(j)\}$$

    3. Repeat step 2 until the number of segments originally lying between points X and O are generated, and compute the Rosenbluth factor W of the new configuration:

$$W = \prod_{i=1}^{l} w_i(n)$$

To restore the symmetry of the Markov chain, we then need to adjust our standard MMC acceptance criterion as follows:
    1. Generate initial configuration (i) using the biased scheme above and compute its Rosenbluth factor W_0
    2. Generate new configuration (ii) using the biased scheme and compute its Rosenbluth factor W_1
    3. Accept the trial move with probability: $\min[1, W_1/W_0]$
    4. Return to step 2 and iterate to equilibrium

So, in order to calculate transition probability between configurations (i) and (ii) in the configurational bias scheme, we need to calculate the ratio of their Rosenbluth factors W_1/W_0.

Hence, starting at X, and remembering that moves that cause chain overlap have infinite energy (*i.e.* zero Boltzmann factor):

$$W_0 = \{\exp(-\beta\varepsilon) + 2\} \cdot 3 \cdot \{\exp(-\beta\varepsilon) + 2\} \cdot \{\exp(-\beta\varepsilon) + 1\} \text{ and}$$

$$W_1 = \{\exp(-\beta\varepsilon) + 2\} \cdot 3 \cdot 3 \cdot \{\exp(-\beta\varepsilon) + 2\}$$

$$\text{Hence } W_1 / W_0 = 3 / \{\exp(-\beta\varepsilon) + 1\}$$

Substituting the numerical values for interaction energy and thermal energy gives $\beta\varepsilon = -2$, which leads to numerical values for acceptance probabilities for standard MMC of: $\exp(-2) = 0.135$ and configuration bias MC: $3/\{\exp(-2)+1\} = 0.358$. The fact that the value for configurational bias MC is higher (which would appear to indicate that configurational bias favours *higher* energy chain conformations, which it does not) is because there is a correspondingly *lower* probability of configuration (ii) being generated as a trial configuration (candidates are not required to prove this). In conventional MMC, the probability of generating configurations (i) and (ii) would be identical. The point is that acceptance probabilities are re-weighted in the former method to restore the symmetry of the Markov chain. If this were not true, then the canonical averages calculated from the biased chain configurations would be inaccurate.

The main advantage of the configurational bias scheme for modelling the flow of an entangled melt of three dimensional polymer chains is that the chain regrowth in a dense melt is a much more efficient way of sampling phase space then generating trial configurations at random, as in the standard MMC method. Thus, less CPU time would be required to achieve equilibration in such a system. However, because chain regrowth is such an inherently *non-local* process, the dynamics of chain motion obtained in the configurational bias simulation would be highly unrealistic compared to the local move set used in the standard MMC algorithm. For example, configurational bias simulations would not be able to reproduce the transition in chain diffusivity scaling with molecular weight from non-entangled to entangled chains. Thus, although MMC methods are generally less efficient at generating configurational properties of the equilibrium state, they would give better data on non-equilibrium properties such as response of system to shear forces.

7. The reaction begins slowly because nucleation requires time and because the particles are at first very small, so that increment of transformation for a unit advance of interface is also small. For the latter reason, the overall rate accelerates as the particles grow. It then decreases as the parent phase available for transformation becomes exhausted.

The results of many isothermal transformation curves can be plotted on a time-temperature-transformation diagram as illustrated in Fig. 6. The curves typically have a *C* shape because the driving force for transformation is small at high temperatures whereas the diffusion coefficient is small at low temperatures. There is an optimum combination of these two parameters at intermediate temperatures, giving a maximum in the rate of reaction. The curve marked 'start' corresponds to a detectable limit of transformation (*e.g.* 5%), and that marked 'finish' corresponds to, say, 95% transformation.
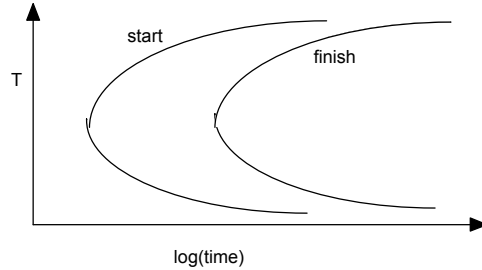
Fig. 6. A time-temperature-transformation (TTT) diagram.

During transformation in extended space, particles can nucleate and grow in all regions irrespective of whether that space represents the parent or product phase.
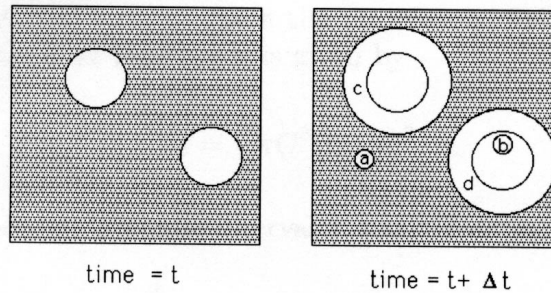
Fig. 7. An illustration of the concept of extended volume. Two precipitate particles have nucleated and grown to a finite size in the time *t*. New regions *c* and *d* are formed as the original particles grow, but *a* & *b* are new particles, of which *b* has formed in a region which is already transformed.

Referring to Fig. 7, suppose that two particles exist at time *t*; a small interval Δt later, new regions marked *a*, *b*, *c* & *d* are formed assuming that they are able to grow unrestricted in extended space whether or not the region into which they grow is already transformed. However, only those components of *a*, *b*, *c* & *d* which lie in previously untransformed matrix can contribute to a change in the real volume of the product phase (α) :

$$dV^{\alpha} = \left(1 - \frac{V^{\alpha}}{V}\right)dV_e^{\alpha} \tag{1}$$

where it is assumed that the microstructure develops at random. The subscript *e* refers to extended volume, V^{α} is the volume of α and V is the total volume. Multiplying the change in extended volume by the probability of finding untransformed regions has the effect of excluding regions such as *b*, which clearly cannot contribute to the real change in volume of the product. For a random distribution of precipitated particles, this equation can easily be integrated to obtain the real volume fraction,

$$\frac{V^{\alpha}}{V} = 1 - \exp\left\{-\frac{V_e^{\alpha}}{V}\right\}$$

A simple modification for the simultaneous formation of two kinds of precipitates (α & β) is that we have a coupled set of two equations,

$$dV^\alpha = \left(1 - \frac{V^\alpha + V^\beta}{V}\right) dV_e^\alpha \text{ and } dV^\beta = \left(1 - \frac{V^\alpha + V^\beta}{V}\right) dV_e^\beta$$

The extended volume V_e^α is straightforward to calculate using nucleation and growth models and neglecting completely any impingement effects. Consider a simple case where the α grows isotropically at a constant rate G and where the nucleation rate per unit volume is I_V. The volume of a particle nucleated at time $t = \tau$ is given by

$$v_\tau = \frac{4}{3} \pi G^3 (t - \tau)^3$$

The change in extended volume over the interval τ and $\tau + d\tau$ is

$$dV_e^\alpha = \frac{4}{3} \pi G^3 (t - \tau)^3 \times I_V \times V \times d\tau$$

On substituting into equation (1) and writing $\xi = V^\alpha/V$, we get

$$dV^\alpha = \left(1 - \frac{V^\alpha}{V}\right) \frac{4}{3} \pi G^3 (t - \tau)^3 I_V V \, d\tau$$

so that $-\ln\{1 - \xi\} = \frac{4}{3} \pi G^3 I_V \int_0^t (t - \tau)^3 d\tau$

and $\xi = 1 - \exp\{-\pi G^3 I_V t^4 / 3\}$